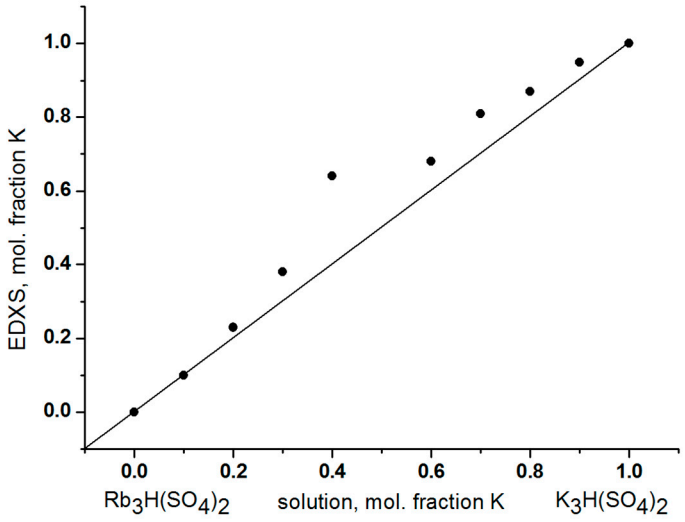

Figure S1. Dependence of the composition of single crystals of solid solutions $(K_xRb_{1-x})_3H(SO_4)_2$ on the composition of the initial solution.

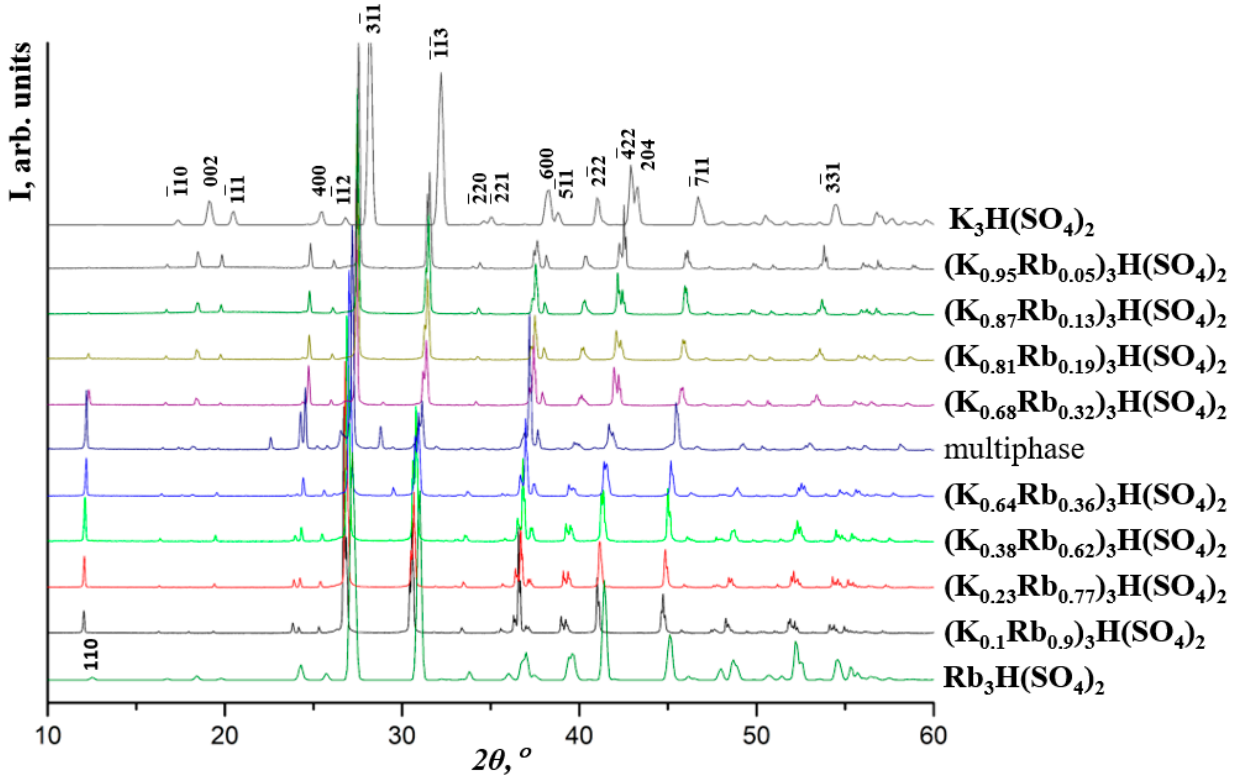

Figure S2. XRD patterns of the $(K_xRb_{1-x})_3H(SO_4)_2$ solid solutions at room temperature. Multiphase sample corresponds to K:Rb = 0.5 solution.

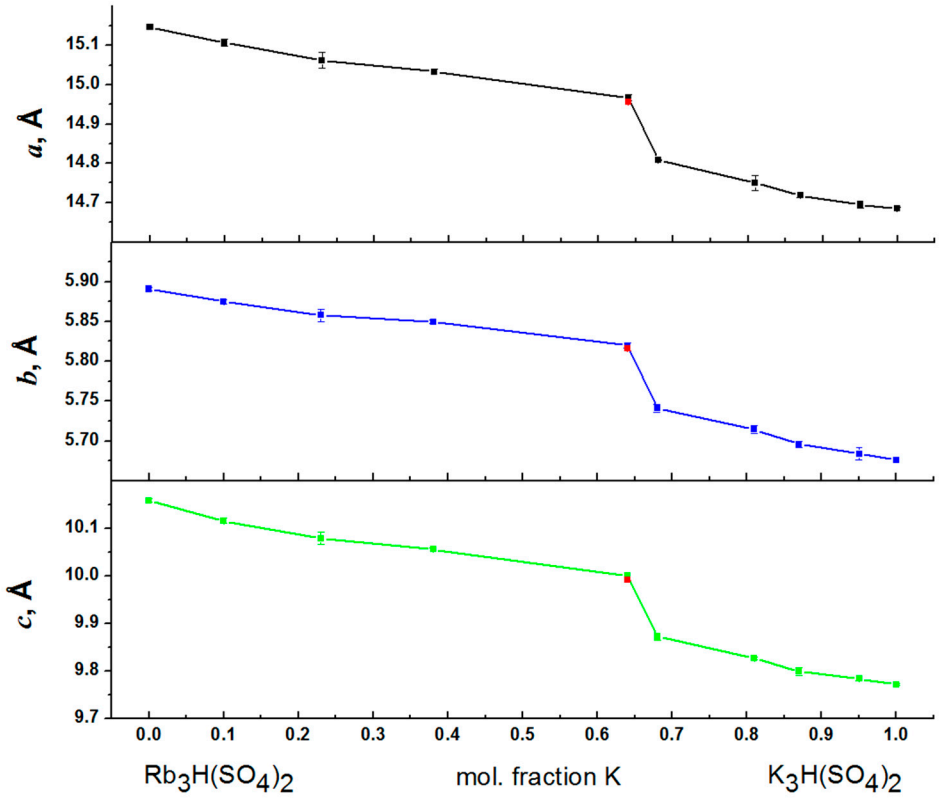

Figure S3. Lattice parameters of $(K_xRb_{1-x})_3H(SO_4)_2$ on composition at room temperature. Red dot responds to the single crystal XRD data.

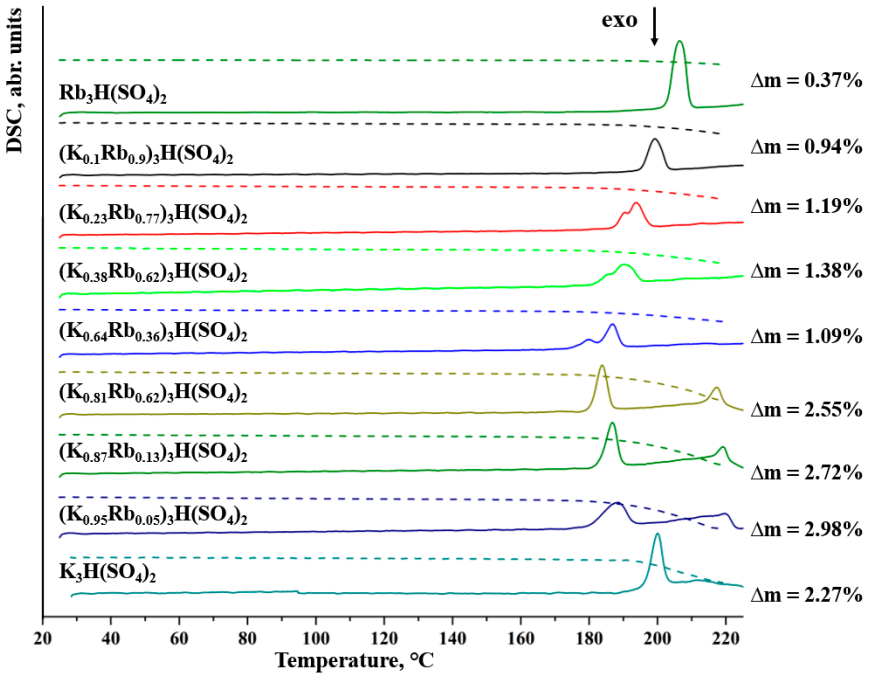

Figure S4. DSC signal and weight loss of $(K_xRb_{1-x})_3H(SO_4)_2$ powders at heating rate 1K/min.

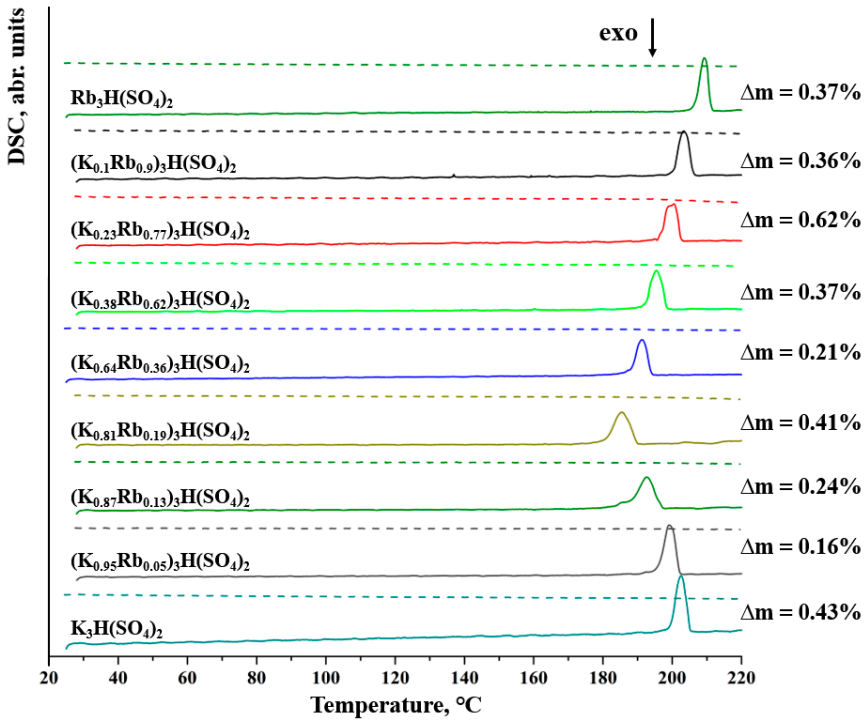

Figure S5. DSC signal and weight loss of $(K_xRb_{1-x})_3H(SO_4)_2$ single crystals at heating rate 1K/min.

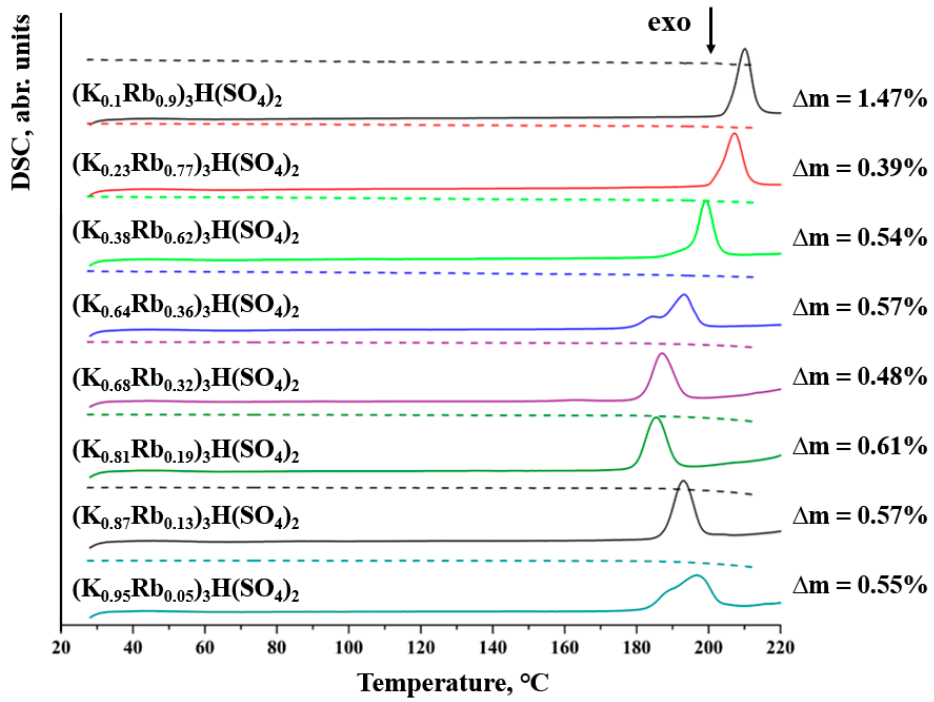

Figure S6. DSC signal and weight loss of $(K_xRb_{1-x})_3H(SO_4)_2$ polycrystalline samples at heating rate 5K/min.

Figures S7-S10 should be commented. The impedance spectra of polycrystalline and single crystal samples, both for the low-temperature monoclinic phase and the high-conductivity state, exhibit nearly identical patterns, as depicted in Figures S8a and S9a, differing only in the electrode contribution. The spectra fitting was performed using equivalent circuits presented in the respective figures. The fitting procedure utilized the elements Rbulk – static bulk conductivity, and CPE - constant phase element. Since the aim was to determine the static bulk conductivity, the electrode contribution was not taken into account (Figure S8) or reduced to CPE element (Figure S9) during the fitting process.

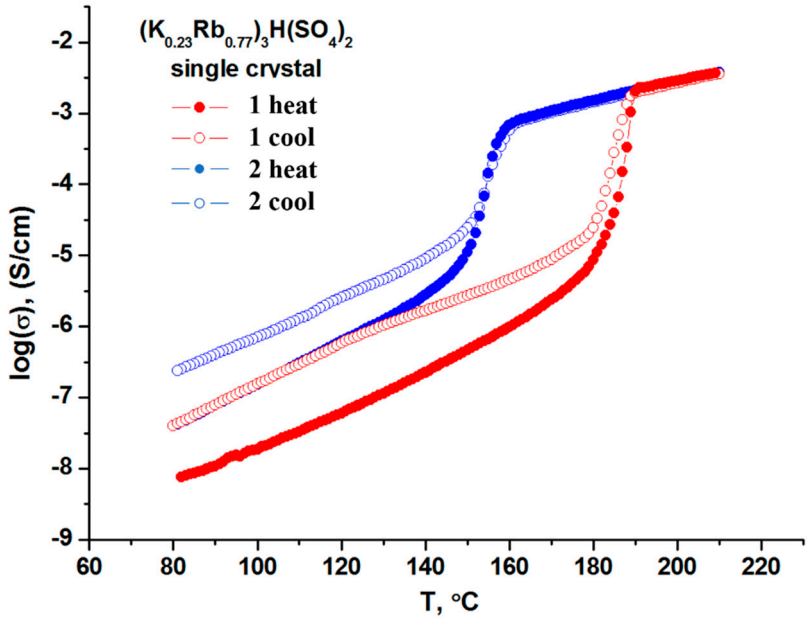

Figure S7. Temperature dependencies of conductivity of the $(K_{0.23}Rb_{0.77})_3H(SO_4)_2$ single crystal in two subsequent heating-cooling cycles.

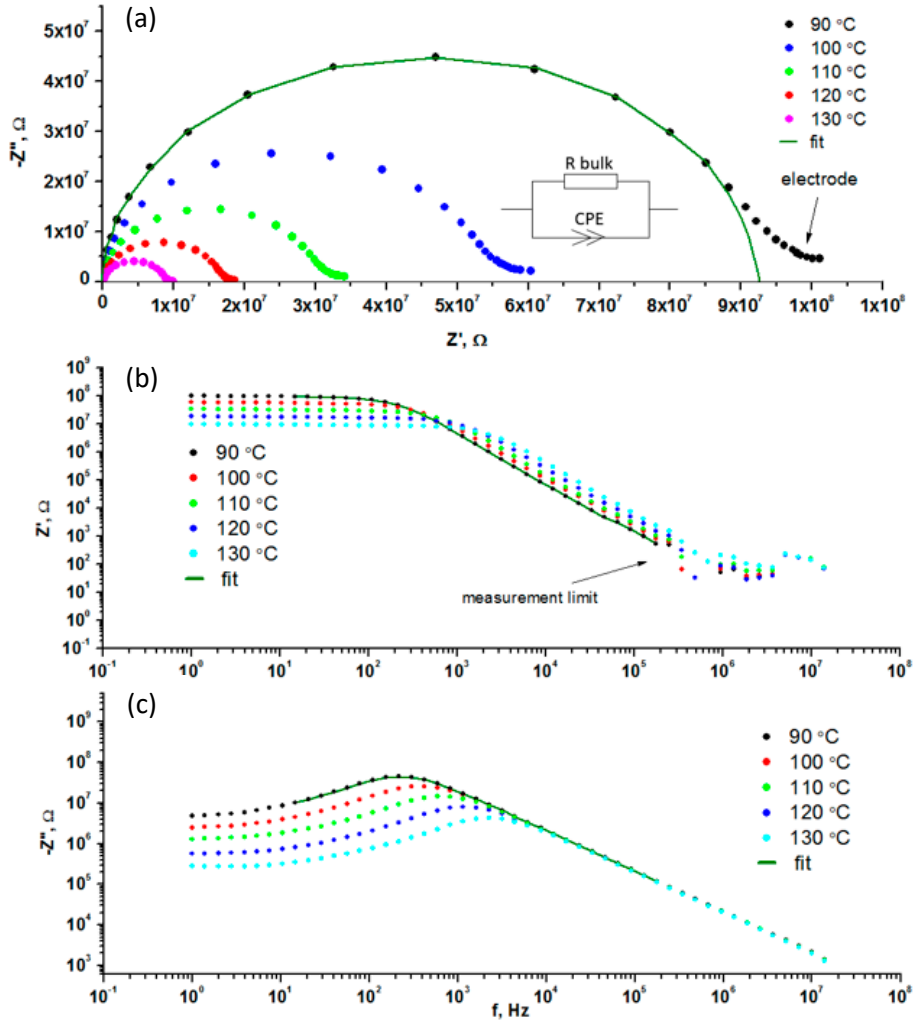

Figure S8. $(K_{0.23}Rb_{0.77})_3H(SO_4)_2$ single crystal. **(a)** Nyquist plots and fits for different temperatures. The complete impedance spectrum is shown in the inset as well as equivalent circuit for fitting; **(b)** and **(c)** Bode plots and fits for different temperatures.

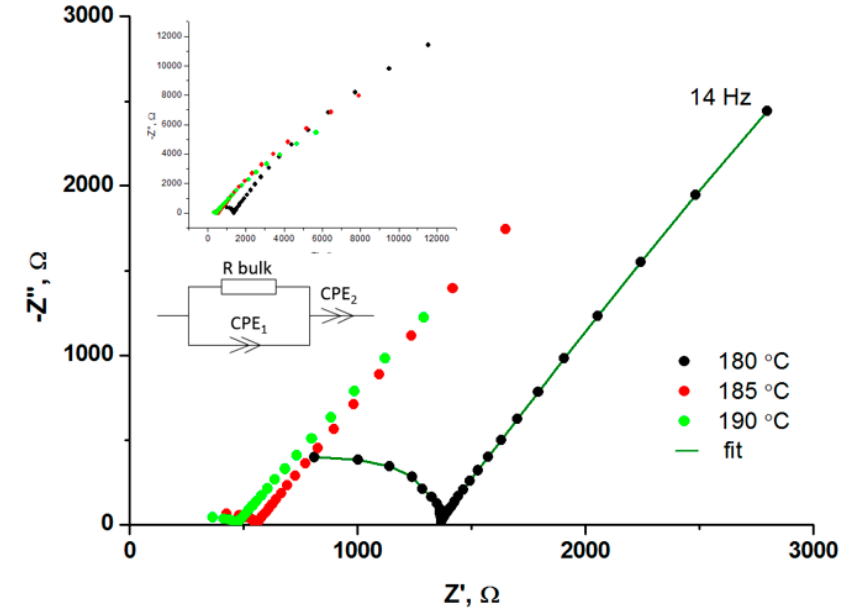

(a)

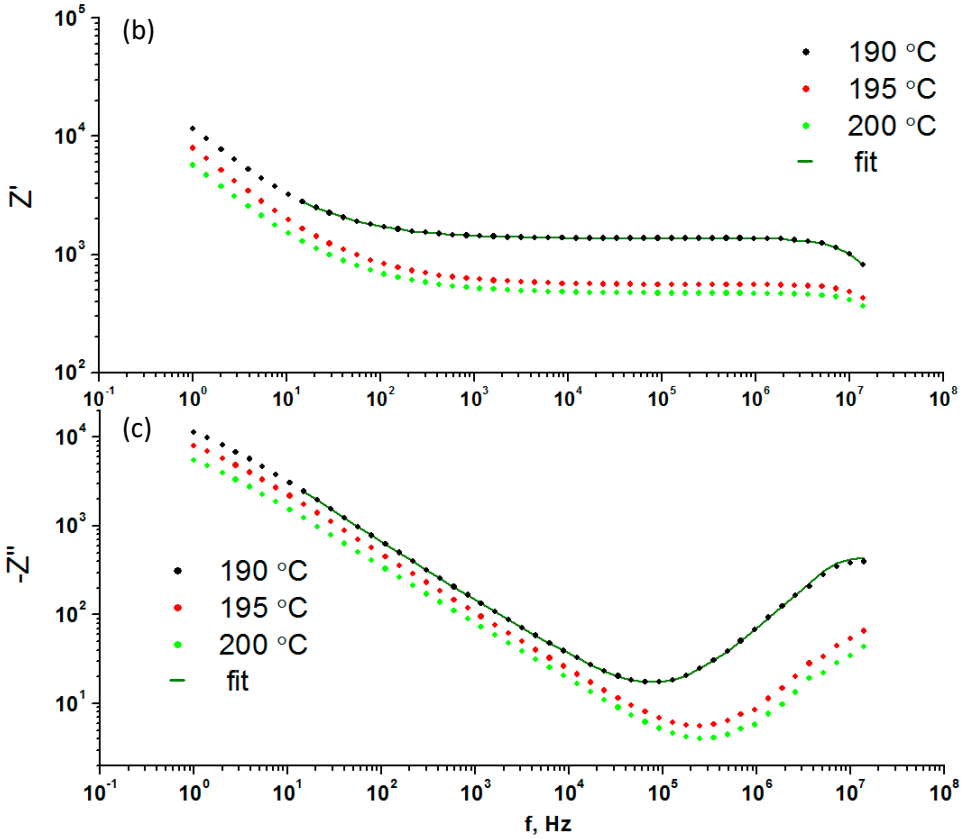

Figure S9. $(K_{0.23}Rb_{0.77})_3H(SO_4)_2$ single crystal. **(a)** Nyquist plots and fits for different temperatures. The complete impedance spectrum is shown in the inset as well as equivalent circuit for fitting; **(b)** and **(c)** Bode plots and fits for different temperatures.

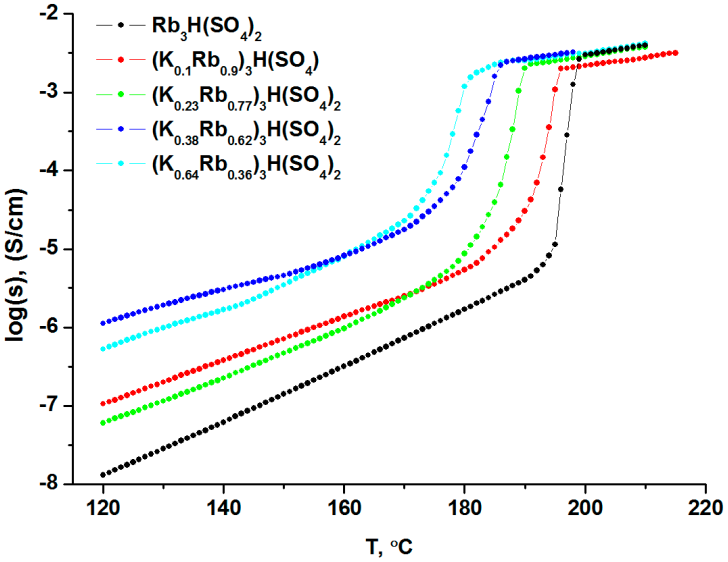

Figure S10. Conductivity of $(K_xRb_{1-x})_3H(SO_4)_2$ (x = 0 – 0.38) single crystals at stepwise heating, mean heating rate was 0.07K/min.

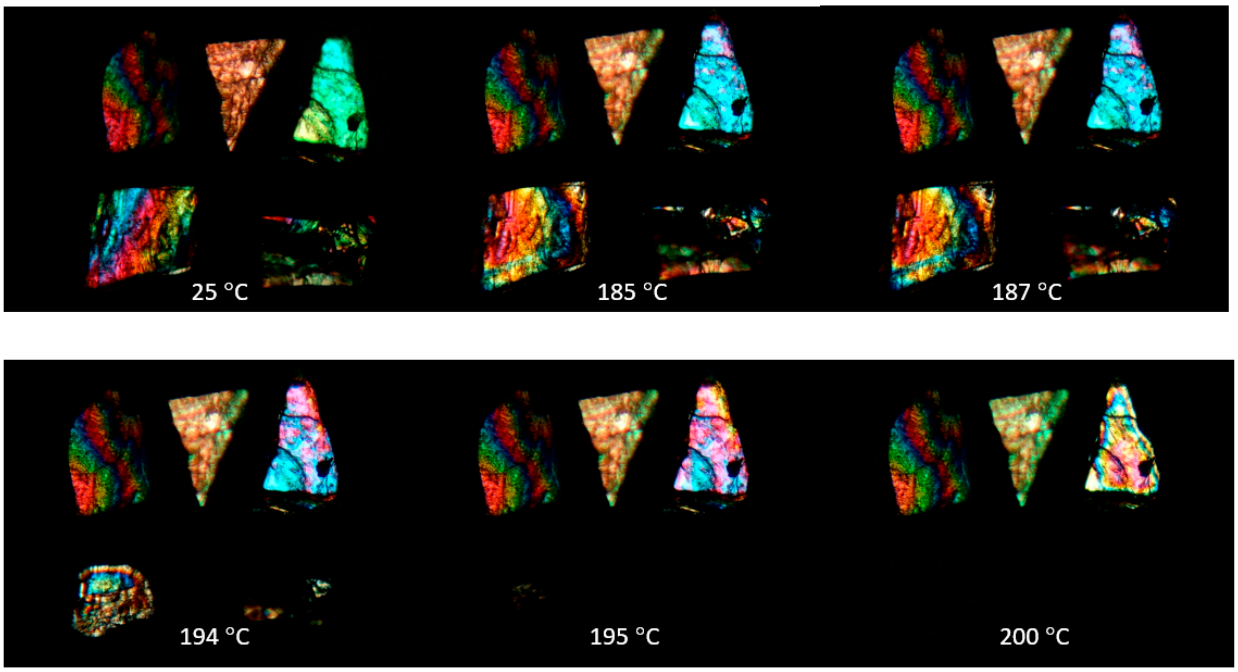

Figure S11. Microphotographs of single crystals $(K_xRb_{1-x})_3H(SO_4)_2$, x = 0 – 0.64, under polarized light, crossed Nicols, at different temperatures. Temperature stabilization time was 15-30 minutes. The values of x are given next to the corresponding crystals.

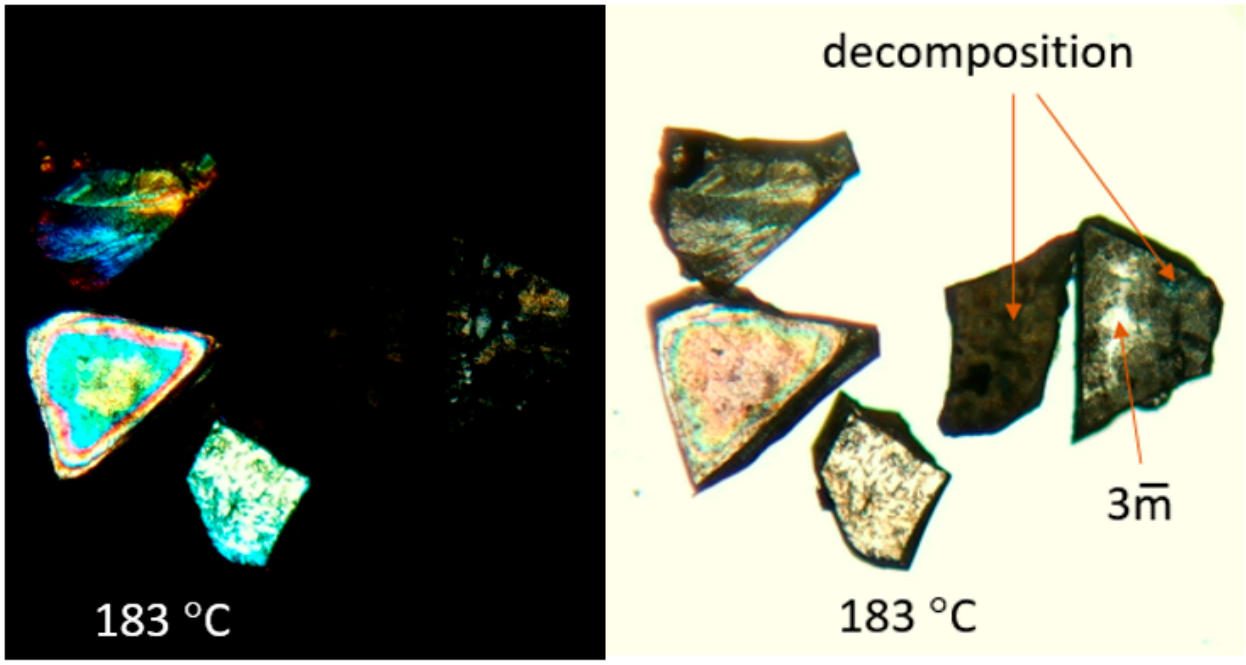

Figure S12. Microphotographs of single crystals $(K_xRb_{1-x})_3H(SO_4)_2$ x = 0.68 − 1 under polarized light.(Crossed Nicols – black background, parallel Nicols - light background). The pictures were taken for the same samples state. Trogonal phase and decomposition rerions are marked by narrows.